

Energy loss measurement for charged particles in very thin silicon layers

This article has been downloaded from IOPscience. Please scroll down to see the full text article.

2011 JINST 6 P06013

(<http://iopscience.iop.org/1748-0221/6/06/P06013>)

View [the table of contents for this issue](#), or go to the [journal homepage](#) for more

Download details:

IP Address: 212.189.159.117

The article was downloaded on 17/11/2012 at 11:36

Please note that [terms and conditions apply](#).

RECEIVED: March 5, 2011

REVISED: May 3, 2011

ACCEPTED: June 14, 2011

PUBLISHED: June 29, 2011

Energy loss measurement for charged particles in very thin silicon layers

S. Meroli,^{a,b,1} D. Passeri^{a,c} and L. Servoli^a

^aINFN — Sezione di Perugia,
via A. Pascoli 1, 06132 Perugia Italy

^bDipartimento di Fisica, Università degli Studi di Perugia,
via A. Pascoli 1, 06100 Perugia, Italy

^cDipartimento di Ingegneria Elettronica e dell'Informazione, Università degli Studi di Perugia,
via Duranti 93, 06100 Perugia, Italy

E-mail: Stefano.Meroli@pg.infn.it

ABSTRACT: The energy loss distribution $f(\Delta)$ of highly relativistic charged particles has been measured for thin silicon layers with thickness ranging from 5.6 to 120 μm . In this work, using an innovative method, the dependence of the energy loss distribution from the thickness of the silicon absorber has been investigated in great detail with reference to CMOS Active Pixel Sensors. The measured energy loss distributions are well-reproduced by calculations also when the target electrons binding energy is taken into account. Finally the results obtained with this method are compared with existing experimental results and theoretical data.

KEYWORDS: Solid state detectors; Particle tracking detectors (Solid-state detectors); Ionization and excitation processes; Detector modelling and simulations I (interaction of radiation with matter, interaction of photons with matter, interaction of hadrons with matter, etc)

¹Corresponding author.

Contents

| | | |
|----------|---|----------|
| 1 | Introduction | 1 |
| 2 | The energy loss distribution theory | 1 |
| 3 | Grazing angle method description | 3 |
| 4 | Experimental setup and data acquisition system | 4 |
| 5 | Data analysis and results | 6 |
| 6 | Conclusions | 9 |

1 Introduction

Solid-state silicon detectors are nowadays widely used in particle physics experiments, e.g. at CERN Large Hadron Collider [1–4], as well as in astroparticle experiments [5, 6]. Fabrication technology advances have enabled the construction of very thin silicon detectors with associated fast read-out electronics. In the future, the requirements for particle tracking systems will be even more stringent, in particular in terms of low material budget and read-out speed [7]. The reduction of the detector thickness decreases the signal rise time, increases the radiation resistance and reduces the material budget and the associated multiple scattering effects. Therefore it is important to investigate the energy loss distribution $f(\Delta)$ due to the passage of ionizing particles through thin layers of matter. To accomplish the $f(\Delta)$ measurement, the charge generated by ionizing particles crossing a silicon layer of known thickness is collected and measured. To perform a comprehensive study, a large number of detectors, each one with different thickness, is needed. This procedure is intrinsically cost and time consuming and very difficult to accomplish, especially for small thicknesses.

In this paper a new method to precisely measure the $f(\Delta)$ at various silicon thicknesses (ranging from 5.6 to 120 μm) is proposed, using only one CMOS Active Pixel Sensor in a grazing angle configuration.

2 The energy loss distribution theory

The statistical nature of the ionizing process during the passage of a fast charged particle through matter results in a large fluctuations of the energy loss (Δ) in an absorber which is thin compared with the particle range. The number of generated electron-hole pairs (J) is related to Δ by the expression $J = P \cdot \Delta$, where P is the average energy needed to produce an electron-hole pair, for the silicon equal to 3.68 eV. Both Δ and J are stochastic quantities. The probability functions $f(\Delta)$ and

$\phi(J)$ are usually called energy loss distribution or straggling function. They may be characterized schematically by the position of the maximum of the distribution function (Δ_p) and the full width at half maximum (w). The Δ_p is located at a lower value compared to the mean energy loss Δ obtained from Bethe-Bloch function. Theoretical calculations of this distribution have been carried out by Landau and Vavilov [8, 9]; these solutions have a different region of applicability and the discriminating parameter is the ratio $k = \Delta E_{\max}$ where E_{\max} is the maximum transferable energy in a single collision.

Landau solved this problem for $k \leq 0.01$ deriving the expected energy loss distribution by solving an integral transport equation:

$$\frac{df}{dx}(x, \Delta) = \int_0^\infty W(E)[f(x, \Delta - E) - f(x, \Delta)]dE. \quad (2.1)$$

Here $f(x, \Delta)$ represents the distribution probability that the incident particle will lose an amount Δ of energy when crossing a layer of thickness x . $W(E)dE$ represents the probability per unit path length of a collision transferring energy E to an electron in the material.

The function $W(E)dE$ is not generally known but Landau was able to derive an approximate solution by using the free electron (Rutherford) cross section:

$$W(E) = \frac{\xi}{x} \cdot \frac{1}{E^2} \quad (2.2)$$

with

$$\frac{\xi}{x} = 0.1535 \frac{z^2 Z}{A \beta^2} \rho = \frac{1.78}{\beta^2} \cdot 10^{-2} \text{keV} \mu\text{m}^{-1} \quad \text{in silicon.} \quad (2.3)$$

In eq. (2.3) z is the charge of incident particle, Z and A are the atomic number and weight of the material and ρ is the density. The Landau distribution is therefore given by

$$f_L(x, \Delta) = \frac{\phi(\lambda)}{\xi} \quad (2.4)$$

with $\phi(\lambda)$ a universal function of the variable λ only

$$\phi(\lambda) = \frac{1}{\pi} \int_0^\infty e^{(-\pi y/2)} \cos(y \ln y + \lambda y) dy \quad (2.5)$$

and

$$\lambda = \frac{\Delta - \langle \Delta \rangle}{\xi} - \beta^2 - \ln(k) - 1 + C_E \quad (2.6)$$

where C_E is the Euler constant equal to 0.5772.

The Landau distribution, $f_L(\Delta)$, is asymmetric with a tail extending to E_{\max} with a maximum for $\lambda = 0.229$ and $w_L = 4.018\xi$.

The energy loss corresponding to the maximum of the function $f_L(\Delta)$ is the most probable energy loss [10]

$${}_L\Delta_p = \xi \left[\ln \frac{2m_e c^2 \beta^2 \gamma^2}{I^2} + \ln \frac{\xi}{I} + 0.2 - \beta^2 - \delta \right] \quad (2.7)$$

where I is the mean excitation potential and δ the density correction.

Subsequently Vavilov derived an improved solution which takes in account the spin of the incident particle. For the collision cross section Vavilov used the form

$$W(E) = \frac{\xi}{x} \cdot \frac{1}{E^2} \left(1 - \frac{\beta^2 E}{E_{\text{MAX}}} \right). \quad (2.8)$$

Vavilov also demonstrated that his solution tends to the Landau function for $k \leq 0.01$, region where Δ is approximated by ξ .

For $k > 10$ the number of collisions is very large and, for the Central Limit Theorem, the Vavilov function coincides with a Gaussian distribution.

Further corrections to the theory taking into account the fact that the electrons in the material are not free have been proposed by Blunck and Leisegang [11], Shulek [12] and Bichsel [13]. For solid-state materials, comparisons with experimental observations have been made: while the most probable energy loss agrees rather well with the prediction of the theory, the width of the distribution is broader than expected and cannot be accounted for by electronic noise or imperfect resolution. The effect is particularly noticeable for very thin absorbers [14], of the order of a few hundred micrometers or less of thickness. The modified energy loss distribution can be improved by using a modified cross section to take into account the electron binding energy.

The modified energy straggling function can be therefore expressed as [15]:

$$f(x, \Delta) = \frac{1}{\sigma \sqrt{2\pi}} \int_{-\infty}^{+\infty} f_L(x, \Delta - \tau) e^{-\frac{\tau^2}{2\delta_2}} d\tau. \quad (2.9)$$

In other words the experimentally observed energy spectrum can be calculated by convolving the Landau distribution with a normal distribution of variance δ_2 . The results of the convolution is a broader distribution with a peak value usually increased by a small amount compared to the Landau theory. Shulek et al. [12] propose the form

$$\delta_2 = \frac{8}{3} \cdot \frac{\xi}{x} \sum_i I_i \cdot f_i \ln \frac{2m_e c^2 \beta^2}{I_i} \quad (2.10)$$

as an estimate of the effect, where I_i is the effective ionization potential of the i -th shell and where f_i is the fraction of electrons in that shell.

3 Grazing angle method description

To accomplish the $f(\Delta)$ measurement for several silicon's thicknesses, without using many detectors, a new method relying only on one CMOS pixel sensor in a grazing angle configuration has been developed [16, 17]. With this configuration, the passage of a charged particle is detected by several pixels pertaining to the single planar detector by forming a track (figure 1). The amount of silicon crossed by the ionizing particle is a function of the particle incident angle, allowing to perform the $f(\Delta)$ characterization at various thicknesses just selecting tracks of different length (detected by the sensor).

From geometrical considerations (figure 2) the particle path (L) through the silicon is related to the incident angle (α) by the expression $L = d / \sin(\alpha)$, where d is the sensitive layer depth of the

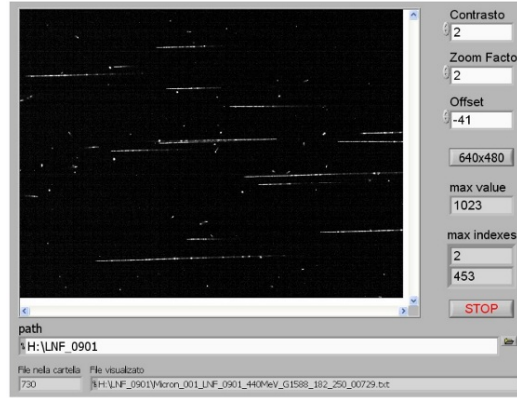


Figure 1. Online display of one recorded frame with several tracks due to 100 MeV electrons.

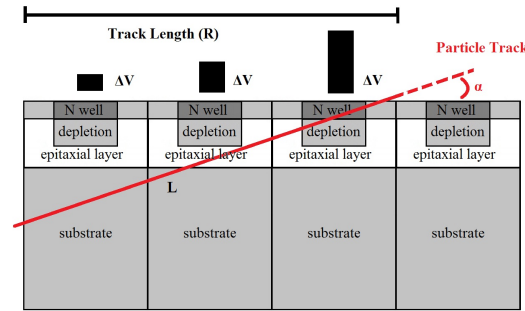


Figure 2. Scheme of grazing angle method: several pixels are hit by the same track.

sensor, and to the measured track length (R) by the expression $L=R/\cos(\alpha)$. The charge released by the ionizing particle is collected by photodiodes where a voltage drop (ΔV) strictly related to the collected charge is produced. The amount of charge collected by the photodiodes depends by the charge generation depth; the deeper the generation point the lower the charge collected, due to the recombination effects.

4 Experimental setup and data acquisition system

A commercial Micron MT9V011 CMOS Sensor (figure 3) [18] featuring $5.6 \times 5.6 \mu\text{m}^2$ pixel size, 640×480 pixels (VGA format) and few micrometers epitaxial layer has been used to perform the measurements. The readout of the sensor is performed by a dedicated read-out board (MT9SH06 evaluation board), with a USB line to power the system, to control the sensor and to receive the data. The high energy resolution (2.5% for 5.9 keV photons) and SNR (~ 30) which can be obtained for minimum ionizing particles with these CMOS sensors [19, 20] suggests their use in precise investigations of the ionization process.

The sensor, together with its special purpose electronics, had a gaussian noise distribution with an independently measured standard deviation σ_{noise} , whose typical value was 32 ± 7 eV. The absolute calibration of the energy scale for the entire system was performed before data taking using a Fe^{55} Xray source.

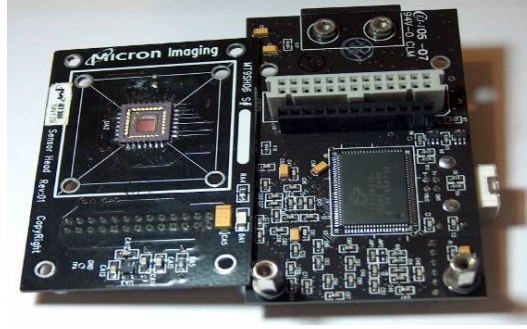


Figure 3. The MT9V011 sensor, the evaluation board (left) and the DAQ board (right).

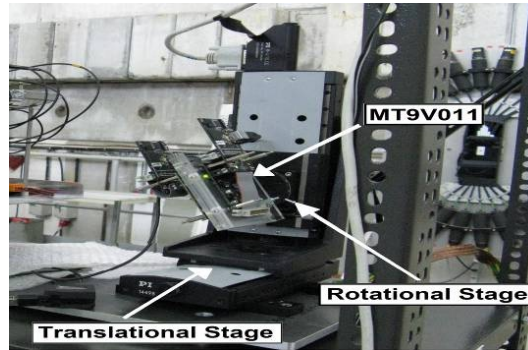


Figure 4. Test Setup at CERN Proton Synchrotron T9 beam line.

The sensor was exposed to 100 MeV electron beam at Laboratori Nazionali di Frascati (LNF), Rome (Italy) and 12 GeV protons at CERN, Geneva (Switzerland) Proton Synchrotron (PS). The sensor has been mounted on a rotational stage, with 1 mrad minimum step (figure 4). The spatial position of the matrix has been chosen as to have the rows almost parallel to the incoming beam direction. The choice of the grazing angle has been dictated by the sensor geometrical constraints in order to have track length up to at least 100 pixels.

These detectors are only partially depleted in the proximity of the n-well/pepi junction and the detector active volume is limited mostly to the epitaxial layer and the charge collection efficiency (CCE) tends to decrease for charge generated within the sensor bulk, because of the high carrier recombination probability inside the p^{++} substrate. Figure 5 shows the CCE profile as a function of the distance from the sensor surface [16].

The profile could be divided roughly in three parts:

1. the first micrometer, where the charge collection efficiency is not complete, due most likely to the presence of the pixel architecture and p-wells regions (hosting the pixel transistors);
2. from $1\ \mu\text{m}$ to $3.5\ \mu\text{m}$, where there is a plateau in efficiency, approximately corresponding to the epitaxial layer;
3. from $3.5\ \mu\text{m}$ to $12\ \mu\text{m}$ where the efficiency decreases due to the increasing distance of the generated charge region from the collecting region.

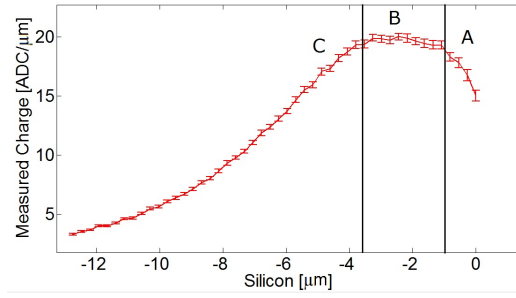


Figure 5. Charge collection efficiency for MT9V011 sensor.

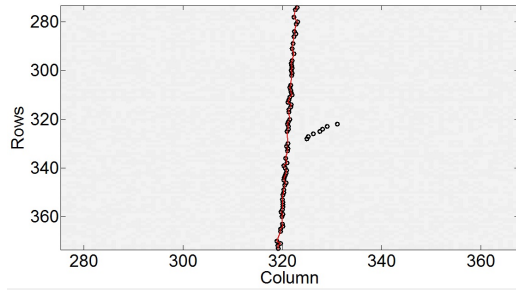


Figure 6. 100 MeV electron track with secondary emission.

The only region used in the investigation of the $f(\Delta)$ is the one ranging from $1 \mu\text{m}$ to $3.5 \mu\text{m}$ in depth (the B region in figure 5), where almost all the generated electron-hole pairs are collected. Because the generation point in this region is close to the photodiodes, the charge diffusion is limited and the charge sharing among pixels belonging to the same track is negligible.

For this study, tracks with different pixel length can be used, knowing that for a longer track there will be more pixels in the B region and then more crossed pixels at maximum CCE. Selecting segments with a different number of pixels it is then possible to build an energy loss function for several silicon thicknesses.

A track finding algorithm has been implemented to select good tracks and to reject background signals (e.g. noisy pixels, short tracks). To obtain a better track spatial definition, for each hit pixel the neighbor pixels in the direction orthogonal to the beam are checked: if their signals are greater than a defined threshold (2 times the pixel noise), the pixels are included in the track. The implemented algorithm allows the separation of different tracks with a distance of only few pixels, as shown in figure 6, where a secondary emission electron could be detected.

5 Data analysis and results

In the present study, energy loss distributions were obtained for 100 MeV electrons and 12 GeV protons. Due to the particle energy used in our investigation, the value of k will be always less than 0.01. Consequently, the observed energy loss distributions are expected to be well represented by eq. (2.9), in which a gaussian function convolves a Landau distribution. The standard deviation σ_{tot}

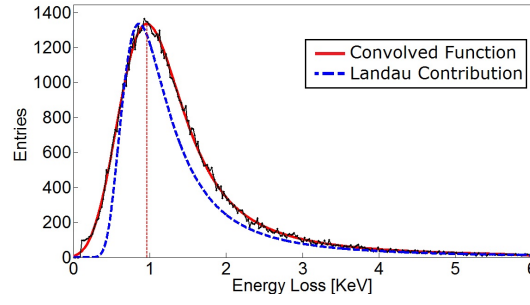


Figure 7. Energy loss distribution for 12 GeV protons passing through 5.6 μm of silicon with convolved function fit and Landau contribution of this fit.

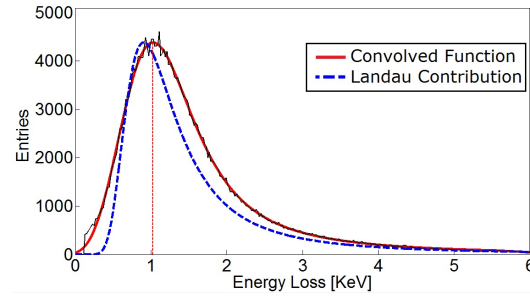


Figure 8. Energy loss distribution for 100 MeV electrons passing through 5.6 μm of silicon with convolved function fit and Landau contribution of this fit.

of the gaussian part should take into account also the detector and electronic noise σ_{noise} :

$$\sigma_{\text{tot}}^2 = \sigma_{\text{noise}}^2 + \delta_2^2 \quad (5.1)$$

Therefore, the experimental energy loss distributions for each momentum and type of particle were fitted to the Landau convolved with a Gaussian with three free fitting parameters: σ_{tot} , ξ and $L\Delta_p$.

In figures 7 and 8 are shown the energy loss distributions for 12 GeV protons and 100 MeV electrons passing through 5.6 μm of silicon.

Superimposed on the experimental data are the energy loss distribution fitted using a convolved function according the eq. (2.9) and a Landau distribution extracted from this fit. Both figures show the importance of electronic binding effects, which tends to broaden the energy loss distribution.

The Δ_p is equal to 0.966 ± 0.035 keV for the 12 GeV protons and 1.018 ± 0.050 keV for 100 MeV electrons, corresponding to 262 ± 10 and 277 ± 14 electron-hole pairs. The extracted value for w is 1.04 ± 0.012 keV for the protons and 1.12 ± 0.018 keV for the electrons while the value for δ_2 is 0.27 ± 0.18 keV for the protons and 0.31 ± 0.23 keV for the electrons.

The shift of the most probable energy loss of the straggling function (Δ_p) respect to $L\Delta_p$ is about 12%. The Landau fit fails to correctly model these experimental data because the theory of Landau assumes that the typical energy loss in an absorber should be large compared to the binding energy of the most tightly bound electron, a condition which is not satisfied for this thickness. In fact for the validity of the Landau approach, ξ should be much more than the atomic binding energy, which means $x/\beta^2 \gg 100 \mu\text{m}$.

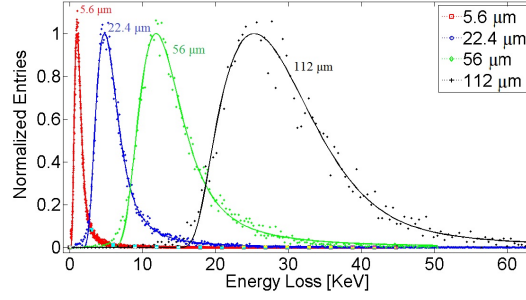


Figure 9. Energy loss distributions with fits for 12 GeV protons passing through several silicon thicknesses.

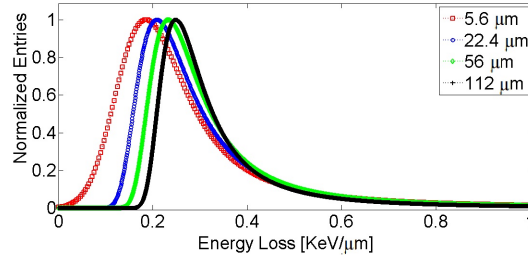


Figure 10. Fit to energy loss per unit length distribution for 12 GeV protons passing through several silicon thicknesses.

Varying the thickness of the silicon absorber the distributions change noticeably. In figure 9 are shown several energy loss distributions obtained for 12 GeV protons in silicon absorbers of different thickness. For each distribution, the fit using eq. (2.9) reproduces well the experimental data.

To better understand the Δ_p dependence from the thickness of crossed silicon, in figure 10 are shown the fits obtained from several distributions of the energy loss per unit length of crossed silicon. The position of the peak of the normalized distributions tends to increase with the silicon thickness, while the distribution broadens for thinner layers. In fact, for small values of k , the Landau width w_L is proportional to the thickness while the width of the convolution Gaussian δ_2 is proportional to $(\text{thickness})^{1/2}$.

In figures 11 and 12 the Δ_p/x as a function of the silicon thickness for respectively 12 GeV protons and 100 MeV electrons is plotted. The blue circles represent the measured values Δ_p/x with their error bars coming from the peak error of the energy loss fit, while the red line represents a logarithmic fit performed on these data according the eq. (2.7).

A very good agreement could be observed in all the studied range (5.6 to 120 μm).

In table 1 we compare the results for specific values of silicon thickness with theoretical predictions and other experimental measurements. The data obtained with the grazing angle method, using 12 GeV proton ($\beta\gamma = 12.3$), are compared with experimental data reported in [21] obtained using pions having a $\beta\gamma$ equal to 14, and with theoretical data reported in [22] obtained by the convolution method for highly relativistic particles.

The general observation is that the results obtained through the grazing angle method closely follow the experimental data and agree with the predicted values within the experimental errors. The small gaussian error σ_{noise} due to the electronic and sensor characteristics allows a precision in the experimental measurements significantly better than the other methods.

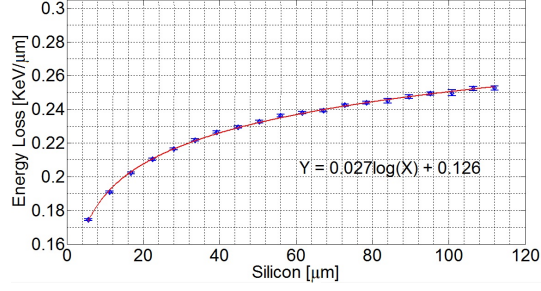


Figure 11. Energy loss for 12GeV protons passing through several silicon thickness.

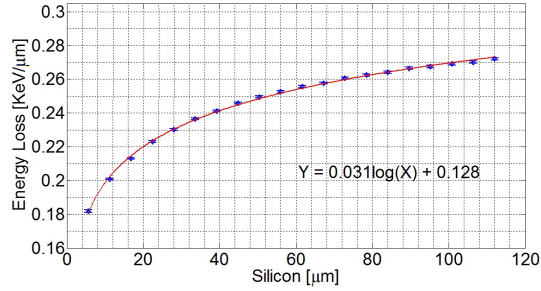


Figure 12. Energy loss for 100MeV electrons passing through several silicon thickness.

Table 1. Comparison between our results obtained with 12 GeV protons and other experimental and theoretical results.

| x [μm] | 32 | 51 | 100 |
|---|-------|--------|--------|
| Δ_p [keV] this work | 7.04 | 11.81 | 24.75 |
| Δ_p [keV] theoretical [22] | 7.092 | 11.840 | 25.283 |
| Δ_p [keV] experimental [21] | 6.91 | 11.79 | 25.96 |
| Δ_p/x [$e-h/\mu\text{m}$] this work | 60 | 63 | 67 |
| w [keV] this work | 4.98 | 7.22 | 13.17 |
| w [keV] theoretical [22] | 5.172 | 7.201 | 12.929 |
| w [keV] experimental [21] | 5.26 | 7.25 | 13.29 |
| σ_{noise} [keV] this work | 0.14 | 0.16 | 0.23 |
| σ_{noise} [keV] experimental [21] | 0.78 | 0.73 | 2.0 |

6 Conclusions

A new method based on a grazing angle technique to measure the energy loss distribution of particle crossing thin silicon layers has been developed. Using this method it is possible to characterize precisely the energy loss distribution for different thicknesses of silicon absorbers ($5.6 \mu\text{m}$ sampling granularity already achieved). Only one sensor with sufficient segmentation is required (e.g. commercial Active Pixel Sensor). The validity of the method has been checked with the expected theoretical distribution and experimental data. It has been possible also to characterize the broadening of the energy loss distribution caused by the increasing influence of the resonance collisions

on the straggling function. The γ -dependence of the energy loss for relativistic particle has been studied. Special emphasis has been placed on the study of Δ_p and w whose values have been measured for many different thicknesses. The low noise of the sensor and its associated electronics allows a significant reduction of the experimental errors on the energy loss measurements.

References

- [1] ATLAS collaboration, *The ATLAS silicon microstrip tracker. Operation and performance*, 2010 *JINST* **5** C12050.
- [2] CMS Collaboration, *Commissioning and performance of the CMS silicon strip tracker with cosmic ray muons*, 2010 *JINST* **5** T03007.
- [3] M. Moritz et al., *Performance study of new pixel hybrid photon detector prototypes for the LHCb RICH counters*, *IEEE Trans. Nucl. Sci.* **NS-51** (2004) 1060.
- [4] ALICE collaboration, *The ALICE experiment at the CERN LHC*, 2008 *JINST* **3** S08002.
- [5] PAMELA collaboration, *PAMELA sub-detectors capability in light nuclei identification*, *J. Phys. Conf. Ser.* **203** (2010) 012132.
- [6] FERMI collaboration, *The Large Area Telescope on the Fermi gamma-ray space telescope mission*, *Astrophys. J.* **697** (2009) 1071 [[arXiv:0902.1089](#)].
- [7] SUPERB collaboration, *The SuperB silicon vertex tracker*, *PoS(RD09)038*..
- [8] L. Landau, *On the energy loss of fast particles by ionization*, *J. Phys. USSR* **8** (1944) 201.
- [9] P. Vavilov, *Ionization losses of high energy heavy particles*, *Sov. Phys. JETP* **5** (1957) 749.
- [10] PARTICLE DATA GROUP collaboration, *Passage of particles through matter*, *Nucl. Part. Phys.* **33** (2006) 258.
- [11] O. Blunck and S. Leisegang, *Zum Energieverlust schneller Elektronen in dünnen Schichten*, *Z. Physik* **128** (1950) 500.
- [12] P. Shulek et al., *Fluctuations of ionization loss*, *Sov. J. Nucl. Phys.* **4** (1967) 400.
- [13] H. Bichsel, *Straggling of heavy charged particles: comparison of Born hydrogenic-wave-function approximation with free-electron approximation*, *Phys. Rev.* **B 1** (1970) 2854.
- [14] H. Esbensen et al., *Random and channeled energy loss in thin germanium and silicon crystals for positive and negative 2–15 GeV/c pions, kaons, and protons*, *Phys. Rev.* **B 18** (1978) 1039.
- [15] S. Hancock et al., *Energy loss and energy straggling of protons and pions in the momentum range 0.7 to 115 GeV/c*, *Phys. Rev.* **A 28** (1983) 615.
- [16] S. Meroli et al., *A grazing angle technique to measure the charge collection efficiency for CMOS active pixel sensors*, in press in *Nucl. Instrum. Meth.* **A** (corrected proof).
- [17] D. Passeri et al., *Tilted CMOS active pixel sensors for particle track reconstruction*, *IEEE Nucl. Sci. Symp. Conf. Rec.* **NSS 09** (2009) 1678.
- [18] Micron Imaging MT9SH06 technical documentation. Revision 2.8.0, (2007).
- [19] L. Servoli et al., *Characterization of standard CMOS pixel imagers as ionizing radiation detector*, 2010 *JINST* **5** P07003.
- [20] L. Servoli et al., *Use of standard CMOS imagers as position detectors for charged particle*, *Nucl. Phys. Poc. Suppl.* **B 215** (2011) 228.

- [21] J.F. Bak et al., *Large departures from Landau distribution for high-energy particles traversing thin Si and Ge targets*, *Nucl. Phys. B* **288** (1987) 681.
- [22] H. Bichsel, *Straggling in thin silicon detectors*, *Rev. Mod. Phys.* **60** (1988) 663.